

Joint constraint on the jet structure from the short GRB population and GRB 170817A

XIAO-FENG CAO,¹ WEI-WEI TAN,¹ YUN-WEI YU,^{2,3} AND ZHEN-DONG ZHANG²

¹Research Center for Astronomy, Hubei University of Education, Wuhan 430205, China; caoxf@mails.cnu.edu.cn, wwtan@hue.edu.cn

²Institute of Astrophysics, Central China Normal University, Wuhan 430079, China, yuyw@ccnu.edu.cn

³Key Laboratory of Quark and Lepton Physics (Central China Normal University), Ministry of Education, Wuhan 430079, China

ABSTRACT

The nearest GRB 170817A provided an opportunity to probe the angular structure of the jet of this short gamma-ray burst (SGRB), by using its off-axis observed afterglow emission. It is investigated that whether the afterglow-constrained jet structures can be consistent with the luminosity of the prompt emission of GRB 170817A. Furthermore, by assuming that all SGRBs including GRB 170817A have the same explosive mechanism and jet structure, we apply the different jet structures into the calculation of the flux and redshift distributions of the SGRB population, in comparison with the observational distributions of the Swift and Fermi sources. As a result, it is found that the single-Gaussian structure can be basically ruled out, whereas the power-law and two-Gaussian models can in principle survive.

Keywords: gamma-ray burst (629)

1. INTRODUCTION

Gamma-ray bursts (GRBs) are generated by highly-beamed relativistic jets, which are driven by rapidly rotating black hole or neutron star engines. Before the gamma-ray emission is produced, the jets should first propagate through dense progenitor material, which can be a stellar envelope for long GRBs (Zhang et al. 2003; Matzner 2003; Lazzati & Begelman 2005; Bromberg et al. 2011, 2014; Suwa & Ioka 2011; Yu 2020; Gottlieb & Nakar 2022; Urrutia et al. 2023a,b) or a merger ejecta for short GRBs (SGRBs; Nagakura et al. 2014; Lazzati et al. 2017; Yu 2020; Hamidani & Ioka 2021; Nathanail et al. 2021; Nativi et al. 2022; Gottlieb & Nakar 2022; Pavan et al. 2022).

As a result of its interaction with the progenitor material, a GRB jet breaking out from the progenitor can finally own an angular structure for its energy and velocity distributions. Generally speaking, the breakout jet can consist of a core region with an opening angle of few degrees and a relatively wider and less energetic wing region (Lazzati et al. 2018; Salafia & Ghirlanda 2022). In addition, the jet can also be surrounded by a much wider cocoon that is contributed by the shocked material. Nevertheless, it seems unnecessary to treat the jet and cocoon separately, due to the mixing of the material and the continuous distribution of the energy. Instead, we can simply treat the cocoon as a part of the jet wing. From the core to the wing, the Lorentz factor and energy density of the jet can decrease quickly with the

increasing angle relative to the jet axis. Three empirical analytical functions have been usually suggested to describe the angular structure of GRB jets, including a power law (Dai & Gou 2001; Zhang & Mészáros 2002; Kumar & Granot 2003; Lazzati & Begelman 2005), a Gaussian (Zhang & Mészáros 2002; Rossi et al. 2002, 2004; Kumar & Granot 2003; Granot & Kumar 2003) and, sometimes, two Gaussians (Tan & Yu 2020; Luo et al. 2022; Wei et al. 2022).

Observational constraints on the jet structures can in principle provide a clue to understand the nature and interior of GRB progenitors. First of all, a direct implication for the angular structure can be derived from the afterglow emission of GRBs, particularly, when the viewing direction deviates from the jet axis significantly (Kumar & Granot 2003). Because of the relativistic beaming effect, the emission from the jet material deviating from the line of sight (LOS) can be detected only after the material is decelerated to have an emission beaming angle larger than the viewing angle. Therefore, it can be expected that the more luminous emission from more energetic jet material can be detected later for an off-axis observation. In this case, the peak of the afterglow light curves can appear when the core emission comes into sight and the increasing light curves before the peak just reflect the angular distribution of the jet energy density.

The problem is, for the majority of observed GRBs, their cosmological distances always prevent us to detect them on a large viewing angle, because of the rapid

decrease of the jet energy with the angle. And, without a GRB trigger, it will be very difficult to capture the orphan afterglow emission of the GRBs. Following such a consideration, the observed GRBs are always assumed to be on-axis and a “top-hat” structure is generally appropriate for the afterglow modelings, at most, by further invoking an opening angle for the jet if a so-called jet break feature appears in the light curves. Nevertheless, this situation has been changed since the detection of the nearest GRB 170817A of a distance of ~ 40 Mpc. The viewing angle of this GRB was quickly constrained to be about $\theta_{\text{obs}} \leq 31^\circ$ by the gravitational wave detection of GW 170817 (Abbott et al. 2017a). This special multi-messenger event provided the first opportunity to constrain the angular structure of the GRB jet by its afterglow emission and various jet structure models had been investigated widely (Lamb & Kobayashi 2017; Xiao et al. 2017; Margutti et al. 2017, 2018; Troja et al. 2017, 2018; D’Avanzo et al. 2018; Lazzati et al. 2018; Mooley et al. 2018; Granot et al. 2018; Resmi et al. 2018; Xie et al. 2018; Nynka et al. 2018; He et al. 2018; Ziaeeepour 2019; Huang et al. 2019; Kathirgamaraju et al. 2019; Lamb et al. 2019; Beniamini & Nakar 2019; Beniamini et al. 2019, 2020; Takahashi & Ioka 2020, 2021; Wei et al. 2022). Besides explaining the afterglow emission, the off-axis observation of GRB 170817A also provides a natural but qualitative explanation for its ultra-low luminosity of $\sim 10^{47} \text{erg s}^{-1}$ (Abbott et al. 2017b; Zhang et al. 2018). Then, it needs to be checked whether the observed prompt luminosity can be quantitatively consistent with the jet structure derived from the afterglow modelings.

Furthermore, a large viewing angle of GRB 170817A is necessary for understanding the very high event rate of nearby GRBs inferred from GRB 170817A. Meanwhile, a question arises here: how can we connect this nearby SGRB rate in a natural way with the rates of the other SGRBs? In more detail, if all SGRBs including GRB 170817A share a common geometry for their jets, then it is crucial to ask how this common jet structure influence our understanding of the observational redshift and energy distributions of all SGRBs as well as the determination of the luminosity function (LF) and event rate of the SGRBs, as previously investigated by Salafia et al. (2020, 2022); Tan & Yu (2020); Luo et al. (2022). Obviously, the random distribution of the viewing angles of SGRBs can lead to different luminosity for different SGRBs, even though their jets are actually identical. Therefore, a flat low-luminosity component would appear in the apparent LF for a top-hat structure assumption, because the LOS for most SGRBs

must not be strictly parallel to the jet axis and the angle-dependence of the luminosity exists even within the jet core region (but not uniform as assumed in the top-hat model). It was then implied that the intrinsic LF corresponding to the distribution of the central luminosity of SGRB jets could be simply described by a single power law (Tan & Yu 2020).

However, in the previous works, the constraints on the jet structure from the GRB 170817A observations and population statistics were usually treated separately, but have not been quantitatively confronted with each other. Therefore, this paper is devoted to investigate the consistency between these two types of observational constraints. In the next section, we briefly introduce the afterglow model and display the constrained model parameters for three typical structure functions. In Section 3, on the one hand, we derive the angular dependence of the equivalent isotropic emission energy ($E_{\gamma, \text{iso}}$) from the energy density (ε) distribution of the jets, in comparison with the prompt luminosity of GRB 170817A. On the other hand, we compare the model-predicted redshift and flux distributions of SGRBs with the observational ones. A summary is given in Section 4.

2. CONSTRAINING JET STRUCTURE BY GRB 170817A

As usual, for calculating the afterglow emission from a structured jet, we can separate the jet into a series of differential rings and consider the dynamical evolution of each ring independently. By ignoring the possible lateral expansion/motion of the jet rings, the dynamical equation can be written as (Huang et al. 1999; Li et al. 2019):

$$\frac{d\Gamma_\theta}{dM_{\text{sw},\theta}} = -\frac{\Gamma_\theta^2 - 1}{M_{\text{ej},\theta} + 2\Gamma_\theta M_{\text{sw},\theta}}, \quad (1)$$

where Γ_θ is the Lorentz factor of the ring of an half-opening angle θ , $M_{\text{ej},\theta}$ and $M_{\text{sw},\theta}$ are the masses per solid angle of the GRB ejecta and the swept-up interstellar medium (ISM), respectively. By denoting the angular distribution of the jet kinetic energy by $\varepsilon_\theta \equiv dE_k/d\Omega$, we can have $M_{\text{ej},\theta} = \varepsilon_\theta/\Gamma_{\theta,i}c^2$, where the subscript “i” of $\Gamma_{\theta,i}$ represents its initial value. Meanwhile, the increase of the swept-up mass is determined by

$$\frac{dM_{\text{sw},\theta}}{dr_\theta} = r_\theta^2 n m_p, \quad (2)$$

where r_θ is the radius of the jet external shock, n is the number density of the ISM, and m_p is the mass of proton.

Following Sari et al. (1998), the synchrotron luminosity contributed by a differential element of a mass $M_{\text{sw},\theta}$

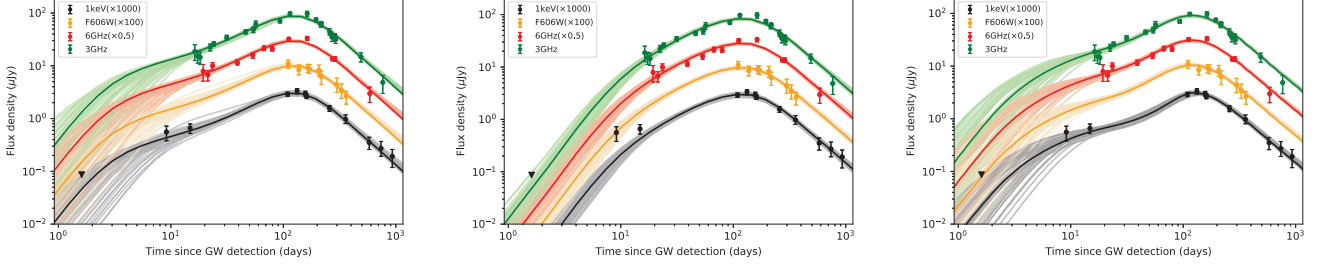


Figure 1. The fits of the multi-wavelength afterglow light curves of GRB 170817A for a power-law (left), single-Gaussian (middle), or two-Gaussian (right) jet structure (Wei et al. 2022).

can be calculated analytically as (Yu et al. 2022)

$$I'_{\nu'}(r, \theta, \varphi) = \frac{M_{\text{sw}, \theta} m_e c^2 \sigma_T B'}{r_\theta^2 m_p} S(\nu'), \quad (3)$$

where the superscript prime indicates the quantities are measured in the comoving frame of the shocked region, m_e is the mass of electron, c the speed of light, σ_T the Thomson cross section, e the electron charge, and B' represents the comoving magnetic field strength. The dimensionless synchrotron spectrum $S(\nu')$ can be expressed as a broken-power-law function, which is characterized by two broken frequencies that are determined by the acceleration and cooling of electrons (see Sari et al. (1998) for details). Then, for an observer of a viewing angle θ_{obs} relative to the jet axis, the observed flux of the afterglow emission can be obtained by integrating over the whole solid angle of the jet as (Huang et al. 2000; Yu et al. 2007, 2022)

$$F_\nu(t) = \frac{r_\theta^2}{d_L^2} \int \frac{I'_{\nu'}(r, \theta, \phi)}{\Gamma_\theta^3 (1 - \beta_\theta \cos \alpha)^3} \cos \alpha d\Omega(\theta, \phi), \quad (4)$$

where d_L is the luminosity distance of the GRB, $\beta_\theta = (1 - \Gamma_\theta^{-2})^{1/2}$, and α is defined as the angle between the emitting differential element and the LOS, which can be expressed as (e.g., Li et al. 2019)

$$\cos \alpha = \cos \theta \cos \theta_{\text{obs}} + \sin \theta \sin \theta_{\text{obs}} \cos \phi. \quad (5)$$

Finally, the connection between the radius of emitting material and the observational time is given by $dr_\theta/dt = \beta_\theta c / (1 - \beta_\theta \cos \alpha)$.

In this paper, the following three representative functions are taken to describe the possible jet structures:

1. Power-law jet

$$\varepsilon_\theta = \varepsilon_c \Theta^{-k_1}, \quad (6)$$

$$\Gamma_{\theta, i} = \Gamma_c \Theta^{-k_2} + 1, \quad (7)$$

with $\Theta = [1 + (\theta/\theta_c)^2]^{1/2}$;

2. Single-Gaussian jet

$$\varepsilon_\theta = \varepsilon_c \exp\left(-\frac{\theta^2}{2\theta_c^2}\right), \quad (8)$$

$$\Gamma_{\theta, i} = \Gamma_c \exp\left(-\frac{\theta^2}{2\theta_c^2}\right) + 1; \quad (9)$$

3. Two-Gaussian jet

$$\varepsilon_\theta = \varepsilon_c \left[\exp\left(-\frac{\theta^2}{2\theta_c^2}\right) + C_E \exp\left(-\frac{\theta^2}{2\theta_{\text{out}}^2}\right) \right], \quad (10)$$

$$\Gamma_{\theta, i} = \Gamma_c \left[\exp\left(-\frac{\theta^2}{2\theta_c^2}\right) + C_\Gamma \exp\left(-\frac{\theta^2}{2\theta_{\text{out}}^2}\right) \right] \quad (11)$$

where the free parameters ε_c , Γ_c , θ_c , C_E , C_Γ , and θ_{out} can be constrained by fitting the observed afterglows of GRB 170817A. To be specific, we substitute these jet structure functions into the dynamical equation and then calculate the afterglow light curves for arbitrary viewing angles. Within a wide range of the model parameters and with the Markov Chain Monte Carlo (MCMC) method, we can constrain the model parameters by comparing the theoretical light curves with the observational data and evaluating their goodness. Finally, the parameter values are listed in Table 1, which are taken from Yu (2020) and Wei et al. (2022). The corresponding fitting results are presented in Figure 1 for a direct impression. Here, the microphysical parameters are defined as usual: p is the spectral index of the shock-accelerated electrons, ϵ_B is the equipartition factor of the magnetic fields in the shocked material and, meanwhile, the equipartition factor for electrons is taken as $\epsilon_e = \sqrt{\epsilon_B}$.

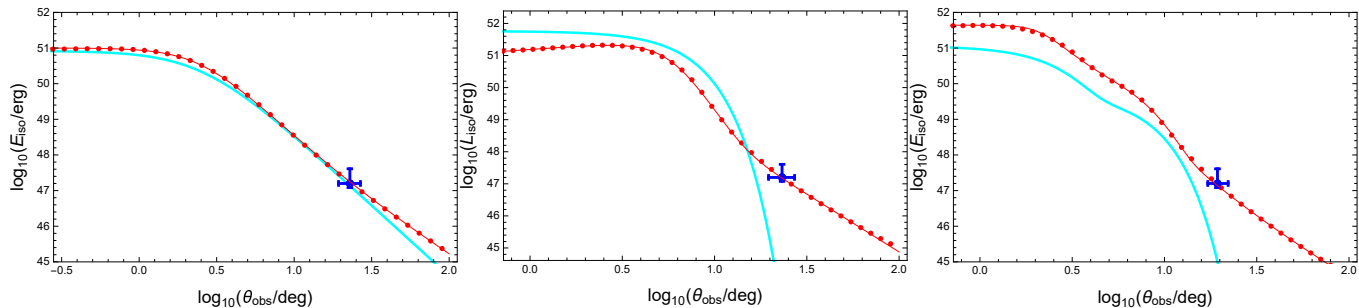
3. CONFRONTING THE JET STRUCTURES WITH THE POPULATION STATISTICS OF SGRBS

3.1. The direction-dependence of the emission energy

Because of the jet structure and the relativistic beaming of the jet emission, the emission energy inferred from observations should highly depend on the viewing angle, which could not always trace the angular distribution of the kinetic energy of the jet (Salafia et al. 2015).

Table 1. Model parameters constrained from the afterglow modeling of GRB170817A.

Parameter	Power-law	Single-Gaussian	Two-Gaussian	Range
$\theta_{\text{obs}}(^{\circ})$	$22.89^{+3.71}_{-3.03}$	$23.21^{+3.95}_{-3.60}$	$19.37^{+2.21}_{-1.53}$	(17, 35)
$\log(\varepsilon_c/\text{erg})$	$50.92^{+0.35}_{-0.54}$	$51.76^{+0.85}_{-0.98}$	$51.04^{+0.24}_{-0.31}$	(48, 53)
$\log(C_E)$	/	/	$-1.33^{+0.19}_{-0.18}$	(-5, 0)
Γ_c	352^{+265}_{-174}	507^{+66}_{-103}	456^{+236}_{-235}	(100, 600)
C_{Γ}	/	/	$0.49^{+0.33}_{-0.30}$	(0, 1)
$\theta_c(^{\circ})$	$2.56^{+1.08}_{-0.62}$	$3.64^{+0.63}_{-0.53}$	$1.48^{+0.41}_{-0.32}$	(1, 10)
$\theta_{\text{out}}(^{\circ})$	/	/	$4.16^{+0.87}_{-0.54}$	(2, 15)
k_1	$3.97^{+0.64}_{-0.52}$	/	/	(3, 8)
k_2	$2.64^{+0.25}_{-0.42}$	/	/	(0.1, 3)
$\log(n/\text{cm}^{-3})$	$-2.98^{+0.49}_{-0.57}$	$-2.06^{+0.94}_{-1.01}$	$-3.19^{+0.40}_{-0.43}$	(-4, 0)
$\log(\epsilon_B)$	$-2.36^{+0.63}_{-0.46}$	$-3.98^{+1.31}_{-1.11}$	$-2.59^{+0.41}_{-0.28}$	(-6, -1)
p	$2.13^{+0.01}_{-0.01}$	$2.12^{+0.01}_{-0.01}$	$2.13^{+0.01}_{-0.01}$	(2, 2.3)

**Figure 2.** The isotropically-equivalent emission energy of SGRBs as a function of viewing angle (solid dots). The angular distribution of the jet kinetic energy are displayed by the gray lines for a comparison. The radiation coefficient η_{γ} can be constrained by according to the observational emission energy of GRB 170817A as shown by the blue data.**Table 2.** Parameters for the empirical description of the $E_{\text{iso}} - \theta_{\text{obs}}$ relation

Model	$L_{\text{on,GRB170817A}}$	θ_{b1}	θ_{b2}	θ_{b3}	s	α_1	α_2	α_3	\mathcal{R}
Power law	51	2.5	18	/	0.6	0.	4.3	1.45	/
Single Gaussian	51.5	6.0	14.3	/	0.4	0.4	9.5	5.9	/
Two Gaussian	51.62	2.1	22.5	3.65	1.4	0.0	4.9	1.75	0.048

Specifically, for a viewing angle θ_{obs} , the isotropically-equivalent energy of the GRB prompt emission can be calculated by (Salafia et al. 2015)

$$E_{\gamma,\text{iso}}(\theta_{\text{obs}}) = \eta_{\gamma} \int \frac{\varepsilon \theta}{\Gamma_{\theta}^4 [1 - \beta_{\theta} \cos \alpha]^3} d\Omega(\theta, \phi), \quad (12)$$

where η_{γ} is the radiation efficiency which is assumed to be a constant for different time and different directions. As shown in Figure 2, we find that the θ_{obs} -dependence

of the emission energy can roughly trace the kinetic energy for viewing angles not much larger than the jet opening angle. However, when the observational direction is far away from the jet axis, the emission energy could become much higher than the kinetic energy at the same direction, particularly, in the Gaussian structure cases. The large angle emission is actually contributed

from the jet material at smaller angles and the prompt

emission of GRB 170817A is just in such a situation¹. By comparing with the isotropic emission energy of GRB 170817A, the radiation efficiency can be constrained to be $\eta_\gamma = 0.08, 0.013,$ and 0.2 for the power-law, single-Gaussian, and two-Gaussian jet structures, respectively.

Furthermore, by taking a constant emission duration of $T \sim 1$ s for all SGRBs and all emission directions, we can connect the observational isotropic luminosity with the emission energy directly as $L_{\text{iso}} = E_{\text{iso}}/T$. Then, the direction-dependence of the isotropic luminosity can be described analytically by the following functions:

$$L_{\text{iso}}(\theta_{\text{obs}}) = L_{\text{on}} \frac{1 + \left(\frac{\theta_{\text{obs}}}{\theta_{b2}}\right)^{\alpha_3}}{\left[\left(\frac{\theta_{\text{obs}}}{\theta_{b1}}\right)^{-\alpha_1 s} + \left(\frac{\theta_{\text{obs}}}{\theta_{b1}}\right)^{\alpha_2 s}\right]^{1/s}}, \quad (13)$$

for the power-law and single-Gaussian jets and

$$L_{\text{iso}}(\theta_{\text{obs}}) = L_{\text{on}} \left\{ \frac{1 + \left(\frac{\theta_{\text{obs}}}{\theta_{b2}}\right)^{\alpha_3}}{\left[\left(\frac{\theta_{\text{obs}}}{\theta_{b1}}\right)^{-\alpha_1 s} + \left(\frac{\theta_{\text{obs}}}{\theta_{b1}}\right)^{\alpha_2 s}\right]^{1/s}} + \mathcal{R} \exp\left(-\frac{\theta_{\text{obs}}^2}{2\theta_{b3}^2}\right) \right\}, \quad (14)$$

for the two-Gaussian jets, which are obtained by fitting the $E_{\text{iso}} - \theta_{\text{obs}}$ relation displayed in Figure 2, where L_{on} is the luminosity value for the on-axis (i.e., $\theta_{\text{obs}} = 0^\circ$) observation.

As found in Salafia et al. (2015) and Tan & Yu (2020), the θ_{obs} -dependence of the GRB luminosity can substantially influence the determination of the LF of SGRBs, which was usually found to have an apparent broken-power-law form (Wanderman & Piran 2015; Ghirlanda et al. 2016; Tan & Yu 2020), where the flat low-luminosity component within the luminosity range ($L_{\text{iso}} \sim 10^{50} - 10^{52} \text{ erg s}^{-1}$) can just be resulted from the angular structure of the jet. Therefore, following Tan & Yu (2020), the intrinsic LF of SGRBs which de-

scribes the probability distribution of the on-axis luminosity L_{on} of different SGRB jets is assumed to have a simple power law form as

$$\Phi(L_{\text{on}}) = \Phi_* \left(\frac{L_{\text{on}}}{L_{\text{on}}^*}\right)^{-\gamma} \exp\left(-\frac{L_{\text{on}}}{L_{\text{on}}^*}\right), \quad (16)$$

where Φ_* is the normalization coefficient. Then, for an observational isotropic luminosity L_{iso} , its detection probability should be calculated by integrating over the arbitrary observational directions as

$$p(L_{\text{iso}}) = \int \Phi(L_{\text{on}}) \sin \theta_{\text{obs}} d\theta_{\text{obs}}, \quad (17)$$

where the fact that the jets can be paired is considered. It is assumed that all SGRB jets have the angular profile identical to that of GRB 170817A, but the total energy of the jets and thus the on-axis luminosity can still be different from each other. In the above integration, the value of L_{on} can be determined by using Eq. (13) or (15) for adopted values of L_{iso} and θ_{obs} .

3.2. Modeling the flux and redshift distributions of SGRBs

For a comparison with the the observational distributions of SGRBs on their fluxes and redshifts, we calculate the model-predicted SGRB numbers in different flux ranges and different redshift ranges by the following integrations (Tan & Yu 2020)

$$N(P_1, P_2) = \Delta\Omega T \int_0^{z_{\text{max}}} \int_{P_1}^{P_2} \eta(P) \times \dot{R}_{\text{SGRB}}(z) p(L_{\text{iso}}) dP \frac{dV(z)}{1+z}, \quad (18)$$

and

$$N(z_1, z_2) = \Delta\Omega T \int_{z_1}^{z_2} \int_0^{P_{\text{max}}} \eta(P) \vartheta_z(z, P) \times \dot{R}_{\text{SGRB}}(z) p(L_{\text{iso}}) dP \frac{dV(z)}{1+z}, \quad (19)$$

respectively, where $\Delta\Omega$ is the field of view of a telescope, T is the working time with a duty cycle of $\sim 50\%$, $\eta(P)$ and $\vartheta(z, P)$ are the trigger efficiency and the probability of redshift measurement, respectively, and $dV(z)$ is the comoving cosmological volume element. The limit values of the redshift z_{max} and the flux P_{max} are taken according to the boundaries of the observational ranges. The isotropic luminosity is calculated by $L_{\text{iso}} = 4\pi d_L^2 P k$, where k is a correction factor that converts the observational photon flux in the detector band to the energy flux in a fixed rest-frame band of $(1, 10^4)$ keV. The most crucial input of the above integrations

¹ Since the single Gaussian cannot directly explain the prompt emission of GRB 170817A, Tan & Yu (2020) suggested an outer Gaussian component. However, as shown here, the GRB 170817A emission actually could be explained by the large-angle emission effect, which indicates the outer Gaussian may be not indispensable. Nevertheless, we keep considering the two-Gaussian situation in this paper, because the two-Gaussian structure could still be a natural result of the jet propagation and it is also helpful for improving the afterglow modeling (Wei et al. 2022).

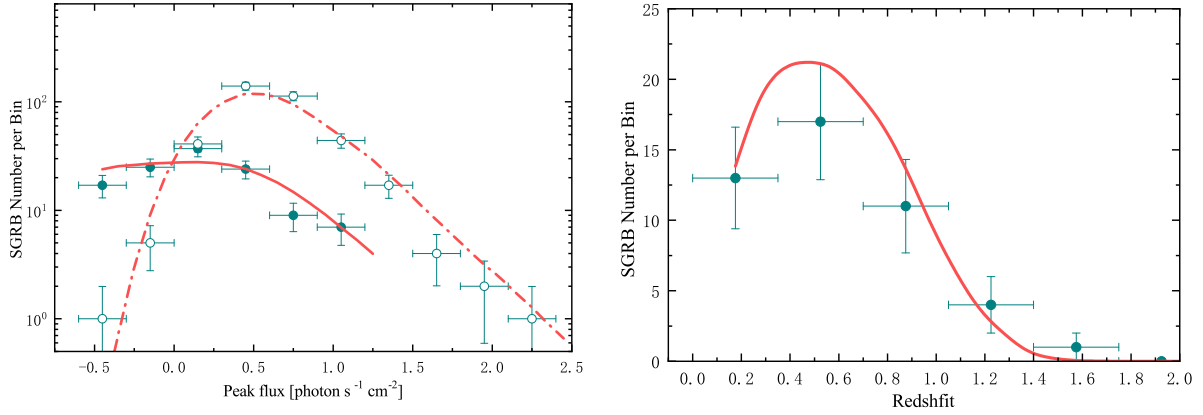


Figure 3. Comparison between the model-predicted and observational flux and redshift distributions of SGRBs for a power-law jet structure. The solid and open data circles are the results of the Swift and Fermi observations, respectively, which are taken from Tan & Yu (2020).

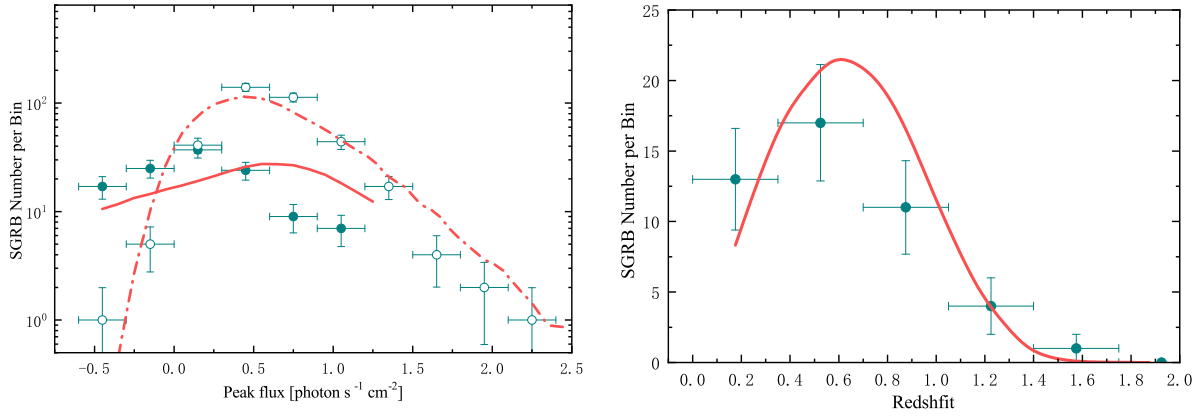


Figure 4. Same to Figure 3 but for a single-Gaussian jet structure.

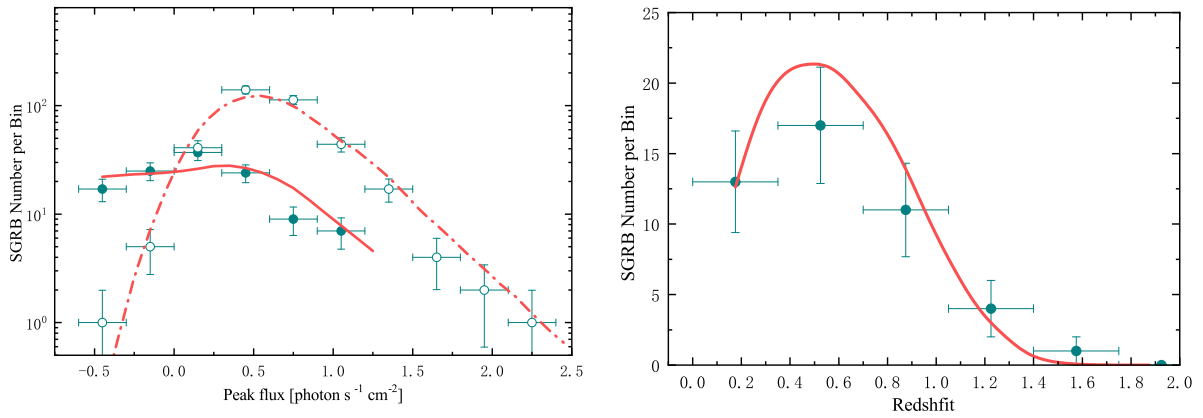


Figure 5. Same to Figure 3 but for a two-Gaussian jet structure.

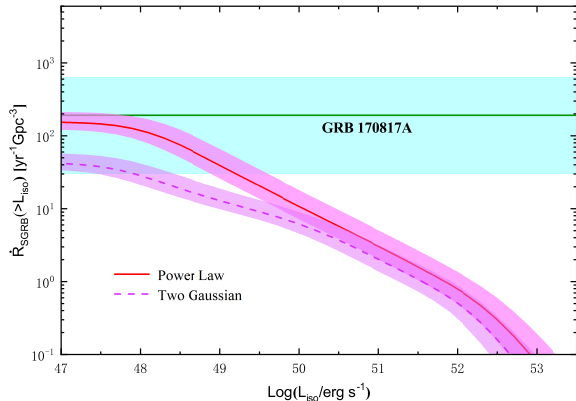


Figure 6. The apparent LF given by the power-law and the two-Gaussian jet models, in comparison with the event rate $190_{-160}^{+440} \text{yr}^{-1} \text{Gpc}^{-3}$ inferred from the GRB 170817A observations represented by the shaded band (Zhang et al. 2018).

is the cosmic rate of SGRBs, which can usually be connected with the cosmic star formation rates (CSFRs) by a delay time since the SGRBs are produced by mergers of compact binaries, where the delay time is determined by the formation process of the compact binaries and the orbital decay through gravitational radiation. By assuming the delay time τ distributes with a probability function $F(\tau)$, we can express the cosmic SGRB rates by (e.g., Regimbau & Hughes 2009; Zhu et al. 2013; Regimbau et al. 2015):

$$\begin{aligned} \dot{R}_{\text{SGRB}}(z) &\propto (1+z) \int_{\tau_{\min}}^{t(z)-t(z_b)} \frac{\dot{\rho}_*[t(z)-\tau]}{1+z[t(z)-\tau]} F(\tau) d\tau \\ &\propto (1+z) \int_{z[t(z)-\tau_{\min}]}^{z_b} \frac{\dot{\rho}_*(z')}{1+z'} F[t(z)-t(z')] \frac{dt}{dz'} dz', \quad (20) \end{aligned}$$

where $\dot{\rho}_*(z)$ is the CSFR, $t(z) = \int_z^\infty [(1+z')H(z')]^{-1} dz'$, $dt/dz = -[(1+z)H(z)]^{-1}$, and z_b represents the redshift at which the binaries started to be formed. Finally, please see Cao et al. (2011) and Tan & Yu (2020) for the details of the expressions of $\eta(P)$, $\vartheta(z, P)$, k , $\dot{\rho}_*(z)$, and $F(\tau)$.

The comparison between the model-predicted distributions with the observational ones are presented in Figures 3, 4, and 5, where the observational data are taken from Tan & Yu (2020). By according to the goodness of the fits presented in Table 3, we can exclude the single-Gaussian model, just as found by Tan & Yu (2020), even though the large-angle emission effect is taken into account in this paper. In comparison, the goodness of the power-law and two-Gaussian models are basically comparable to each other, but the latter one is still relatively better. With the obtained values of the intrinsic LF parameters, the typical delay time, and the total rates of SGRBs, we plot the luminosity dependence of the event

rates of SGRBs (e.g., the apparent LF) in Figure 6, in comparison with the event rate of $190_{-160}^{+440} \text{yr}^{-1} \text{Gpc}^{-3}$ inferred by GRB 170817A (Zhang et al. 2018). As shown, the power-law structure can determine an event rate for $L_{\text{iso}} \gtrsim 10^{47} \text{erg s}^{-1}$ well consistent with the central value of the GRB 170817A rate, whereas the two-Gaussian model can only reach the marginal value of the error range.

4. SUMMARY

The uncovering of the jet structure is one of the most crucial aims of the GRB researches, which can help to understand the nature of their progenitors and central engines. It has been long expected to constrain the jet structure by using the observed afterglow emission. However, usually, only an effective half-opening angle of the jet can be derived from the data, if a so-called jet break characteristic can be identified from the afterglow light curves. The discovery of GRB 170817A had changed this awkward situation, because it was observed off-axis significantly. Then, an immediate question is that whether the jet structures inferred from the afterglows of GRB 170817A can be compatible with the statistical properties of the SGRB population, if it is assumed all SGRBs including GRB 170817A have a common origin and explosive mechanism. Therefore, in this paper, we investigate three typical empirical jet structures including the power-law, single-Gaussian, and two-Gaussian cases, the parameters of which are firstly constrained by according to the afterglow data of GRB 170817A. It is further demonstrated that these three types of jet structures can all account for the prompt luminosity of GRB 170817A, with the consideration of the large-angle emission effect of relativistic jets. However, the single-Gaussian structure is failed to reproduce the redshift and flux distributions of SGRBs, in particular, for the Swift data. By comparison, the power-law structure is most favored by the statistical results and, furthermore, predicts an event rate closest to the value inferred from GRB 170817A.

ACKNOWLEDGMENTS

This work is supported by the National Key R&D Program of China (2021YFA0718500), the China Manned Spaced Project (CMS-CSST-2021-A12), the National Natural Science Foundation of China (grant Nos. 11833003 and U1838203), Hubei Provincial Outstanding Young and Middle-aged Science and Technology Innovation Team Project of China (T2021026), and the Key Laboratory Opening Fund (MOE) of China (grant No. QLPL2021P01).

Table 3. Constraints on the luminosity function and event rates of SGRBs

Model	γ	L_{on}^* [$10^{52} \text{ erg s}^{-1}$]	τ_{min} [Gyr]	$\dot{R}_{\text{SGRB}}(0)$ [$\text{yr}^{-1} \text{ Gpc}^{-3}$]	$P_{\text{KS},F}^{\text{Fermi}}$	$P_{\text{KS},F}^{\text{Swift}}$	$P_{\text{KS},z}$
Power law	$2.54_{-0.22}^{+0.27}$	$5.17_{-0.80}^{+1.14}$	$3.55_{-0.15}^{+0.15}$	$398.48_{-52.42}^{+88.10}$	0.089	0.076	0.267
Single Gaussian	$2.50_{-0.17}^{+0.20}$	$49.1_{-6.7}^{+6.8}$	$3.52_{-0.15}^{+0.10}$	$127.52_{-7.74}^{+60.28}$	4.24×10^{-3}	2.01×10^{-23}	0.005
Two Gaussian	$2.56_{-0.22}^{+0.27}$	$2.00_{-0.30}^{+0.34}$	$3.51_{-0.18}^{+0.14}$	$541.24_{-68.38}^{+128.18}$	0.103	0.269	0.234

REFERENCES

- Abbott, B. P., Abbott, R., Abbott, T., et al. 2017a, PRL, 119, 161101
- Abbott, B. P., Abbott, R., Abbott, T. D., et al. 2017b, *Astrophysical Journal*, 848, L13
- Beniamini, P. & Nakar, E. 2019, MNRAS, 482, 5430. doi:10.1093/mnras/sty3110
- Beniamini, P., Petropoulou, M., Barniol Duran, R., et al. 2019, MNRAS, 483, 840
- Beniamini, P., Granot, J., & Gill, R. 2020, MNRAS, 493, 3521. doi:10.1093/mnras/staa538
- Bromberg, O., Granot, J., Lyubarsky, Y., et al. 2014, MNRAS, 443, 1532
- Bromberg, O., Nakar, E., Piran, T., et al. 2011, *Astrophysical Journal*, 740, 100
- Cao, X.-F., Yu, Y.-W., Cheng, K. S., et al. 2011, MNRAS, 416, 2174
- Dai, Z. G., & Gou, L. J. 2001, *Astrophysical Journal*, 552, 72
- D’Avanzo, P., Campana, S., Salafia, O. S., et al. 2018, A&A, 613, L1. doi:10.1051/0004-6361/201832664
- Ghirlanda, G., Salafia, O. S., Pescalli, A., et al. 2016, A&A, 594, A84
- Granot, J., Gill, R., Guetta, D., et al. 2018, MNRAS, 481, 1597. doi:10.1093/mnras/sty2308
- Granot, J. & Kumar, P. 2003, *Astrophysical Journal*, 591, 1086. doi:10.1086/375489
- Gottlieb, O. & Nakar, E. 2022, MNRAS, 517, 1640. doi:10.1093/mnras/stac2699
- Hamidani, H. & Ioka, K. 2021, MNRAS, 500, 627. doi:10.1093/mnras/staa3276
- He, X.-B., Tam, P.-H. T., & Shen, R.-F. 2018, *Research in Astronomy and Astrophysics*, 18, 043. doi:10.1088/1674-4527/18/4/43
- Huang, Y. F., Dai, Z. G., Lu, T. 1999, MNRAS, 309, 513
- Huang, B.-Q., Lin, D.-B., Liu, T., et al. 2019, MNRAS, 487, 3214. doi:10.1093/mnras/stz1426
- Huang, Y. F., Gou, L. J., Dai, Z. G., et al. 2000, *Astrophysical Journal*, 543, 90. doi:10.1086/317076
- Kathirgammaraju, A., Tchekhovskoy, A., Giannios, D., et al. 2019, MNRAS, 484, L98. doi:10.1093/mnras/ltz012
- Kumar, P., & Granot, J. 2003, *Astrophysical Journal*, 591, 1075
- Lamb, G. P., Lyman, J. D., Levan, A. J., et al. 2019, *Astrophysical Journal*, 870, L15. doi:10.3847/2041-8213/aaf96b
- Lamb, G. P., & Kobayashi, S. 2017, MNRAS, 472, 4953
- Lazzati, D., López-Cámara, D., Cantiello, M., et al. 2017, *Astrophysical Journal*, 848, L6. doi:10.3847/2041-8213/aa8f3d
- Lazzati, D., Perna, R., Morsony, B. J., et al. 2018, PhRvL, 120, 241103
- Lazzati, D. & Begelman, M. C. 2005, *Astrophysical Journal*, 629, 903. doi:10.1086/430877
- Li, Y.-S., Chen, A., & Yu, Y.-W. 2019, *Research in Astronomy and Astrophysics*, 19, 115. doi:10.1088/1674-4527/19/8/115
- Luo, J.-W., Li, Y., Ai, S., et al. 2022, MNRAS, 516, 1654. doi:10.1093/mnras/stac2279
- Margutti, R., Berger, E., Fong, W., et al. 2017, *Astrophysical Journal*, 848, L20
- Margutti, R., Alexander, K. D., Xie, X., et al. 2018, *Astrophysical Journal*, 856, L18
- Matzner, C. D. 2003, MNRAS, 345, 575
- Mooley, K. P., Frail, D. A., Dobie, D., et al. 2018, *Astrophysical Journal*, 868, L11. doi:10.3847/2041-8213/aaeda7
- Nagakura, H., Hotokezaka, K., Sekiguchi, Y., et al. 2014, *Astrophysical Journal*, 784, L28
- Nathanail, A., Gill, R., Porth, O., et al. 2021, MNRAS, 502, 1843. doi:10.1093/mnras/stab115
- Nativi, L., Lamb, G. P., Rosswog, S., et al. 2022, MNRAS, 509, 903. doi:10.1093/mnras/stab2982

- Nynka, M., Ruan, J. J., Haggard, D., et al. 2018, *Astrophysical Journal* , 862, L19.
doi:10.3847/2041-8213/aad32d
- Pavan, A., Ciolfi, R., Vijay Kalinani, J., et al. 2022, arXiv:2211.10135. doi:10.48550/arXiv.2211.10135
- Regimbau, T., Siellez, K., Meacher, D., et al. 2015, *Astrophysical Journal* , 799, 69
- Regimbau, T., & Hughes, S. A. 2009, *Phys. Rev. D* , 79, 062002
- Resmi, L., Schulze, S., Ishwara-Chandra, C. H., et al. 2018, *Astrophysical Journal* , 867, 57.
doi:10.3847/1538-4357/aae1a6
- Rossi, E. M., Lazzati, D., Salmonson, J. D., et al. 2004, *MNRAS* , 354, 86
- Rossi, E., Lazzati, D., & Rees, M. J. 2002, *MNRAS* , 332, 945. doi:10.1046/j.1365-8711.2002.05363.x
- Salafia, O. S., Ghisellini, G., Pescalli, A., et al. 2015, *MNRAS* , 450, 3549. doi:10.1093/mnras/stv766
- Salafia, O. S., Barbieri, C., Ascenzi, S., et al. 2020, *A&A* 636, A105
- Salafia, O. S. & Ghirlanda, G. 2022, *Galaxies*, 10, 93.
doi:10.3390/galaxies10050093
- Salafia, O. S., Colombo, A., Gabrielli, F., et al. 2022, *A&A* , 666, A174. doi:10.1051/0004-6361/202243260
- Sari, R., Piran, T., & Narayan, R. 1998, *Astrophysical Journal* , 497, L17. doi:10.1086/311269
- Suwa, Y., & Ioka, K. 2011, *Astrophysical Journal* , 726, 107
- Takahashi, K. & Ioka, K. 2021, *MNRAS* , 501, 5746.
doi:10.1093/mnras/stab032
- Takahashi, K. & Ioka, K. 2020, *MNRAS* , 497, 1217.
doi:10.1093/mnras/staa1984
- Tan, W.-W., & Yu, Y.-W. 2020, *ApJ*, 902, 83
- Troja, E., Piro, L., van Eerten, H., et al. 2017, *Nature* , 551, 71
- Troja, E., Piro, L., Ryan, G., et al. 2018, *MNRAS* , 478, L18
- Urrutia, G., De Colle, F., Moreno, C., et al. 2023a, *MNRAS* , 518, 5242. doi:10.1093/mnras/stac3433
- Urrutia, G., De Colle, F., & López-Cámara, D. 2023b, *MNRAS* , 518, 5145. doi:10.1093/mnras/stac3401
- Wanderman, D. & Piran, T. 2015, *MNRAS*, 448, 3026
- Wei, F., Zhang, Z.-D., Yu, Y.-W., et al. 2022, *Scientia Sinica Physica, Mechanica & Astronomica*, 52, 129511.
doi:10.1360/SSPMA-2022-0120
- Xiao, D., Liu, L.-D., Dai, Z.-G., et al. 2017, *Astrophysical Journal* , 850, L41. doi:10.3847/2041-8213/aa9b2b
- Xie, X., Zrake, J., & MacFadyen, A. 2018, *Astrophysical Journal* , 863, 58. doi:10.3847/1538-4357/aacf9c
- Yu, Y.-W. 2020, *Astrophysical Journal* , 897, 19
- Yu, Y. W., Liu, X. W., & Dai, Z. G. 2007, *Astrophysical Journal* , 671, 637. doi:10.1086/522829
- Yu, Y.-W., Gao, H., Wang, F.-Y., et al. 2022, *Handbook of X-ray and Gamma-ray Astrophysics*. Edited by Cosimo Bambi and Andrea Santangelo, 31.
doi:10.1007/978-981-16-4544-0_126-1
- Zhang, B., & Mészáros, P. 2002, *Astrophysical Journal* , 571, 876
- Zhang, W., Woosley, S. E., & MacFadyen, A. I. 2003, *Astrophysical Journal* , 586, 356. doi:10.1086/367609
- Zhang, B.-B., Zhang, B., Sun, H., et al., 2018, *Nat. Co.*, 9, 447
- Zhu, X.-J., Howell, E. J., Blair, D. G., et al. 2013, *MNRAS* , 431, 882
- Ziaepour, H. 2019, *MNRAS* , 490, 2822.
doi:10.1093/mnras/stz2735